ANALYSIS OF NON-FOURIER HEAT CONDUCTION IN CONICAL PIN FINS THROUGH THE GENERALIZED INTEGRAL TRANSFORM TECHNIQUE

Carlos Alexandre Moreira da Silva
Carlos Célio Sousa da Cruz
Emanuel Negrão Macêdo
João Nazareno Nonato Quaresma
School of Chemical Engineering, ITEC, Universidade Federal do Pará, UFPA
Campus Universitário do Guamá, 66075-110, Belém, PA, Brazil; quaresma@ufpa.br.

Renato Machado Cotta
Mechanical Engineering Department – POLI/COPPE, Universidade Federal do Rio de Janeiro, UFRJ
Cx. Postal 68503 – Cidade Universitária, 21945-970, Rio de Janeiro, RJ, Brazil; cotta@mecanica.coppe.ufrj.br.

Abstract. *The Generalized Integral Transform Technique (GITT) is employed in the hybrid solution of energy equation to describe the non-fourier heat conduction behavior of conical pin fins. The employment of the GITT approach in the hyperbolic heat conduction equation leads to a coupled system of second order ordinary differential equations in the time. Therefore, this resulting system is then numerically solved by using the Gear`s method for stiff problems, available in the subroutine DIVPAG from the IMSL Library. Numerical results for the temperature field is computed for different Biot numbers and dimensionless thermal relaxation times, which are then compared with those previously reported in the literature for special cases.*

Keywords*: Hyperbolic heat conduction, Conical pin fins, Integral transform.*

1. INTRODUCTION

The phenomenon of finite speed of thermal propagation has gained much attention along the years, mainly due to special applications that can not be modeled by the classical Fourier model; among them one can cite pulsating laser heating, rapidly contacting surfaces in electronic devices and heat transfer in nanosystems.

Several models have been proposed in the literature to describe such hyperbolic behavior, therefore the Cattaneo-Vernotte model (Cattaneo, 1958; Vernotte, 1958) is the more spread one, although some authors may point out some limitations in it because of a possible violation of the second law of thermodynamics (Criado-Sancho and Llebot, 1993; Bai and Lavine, 1995).

Many authors have analyzed the non-Fourier Cattaneo-Vernotte model for heat transfer in fast processes (Tsai et al., 2005; Quaresma et al., 2001; Cruz et al., 2001; Macêdo et al., 2005), but particularly in dealing with heat conduction in fins one cites works of Lin (1998) who studied the effect of the relaxation time on the performance of a convective fin of constant cross-sectional area subjected to periodic thermal conditions, by employing a hybrid scheme involving the Laplace transform and the finite volume method and that of Silva et al. (2006) who analyzed the same problem by employing the Generalized Integral Transform Technique (GITT).

In this context, following the same steps in the previous work of Silva et al. (2006), the main objective of the present work is to develop a hybrid numerical-analytical solution based on the GITT approach (Cotta, 1993; Cotta, 1994; Cotta and Mikhailov, 1997; Cotta and Mikhailov, 2006) to analyze the non-Fourier thermal response of a conical pin fin by using the Cattaneo-Vernotte model, such as that one studied by Cotta et al. (1993), where it was used the Fourier model. The employment of the GITT approach to solve the related hyperbolic partial differential equation produces a fast and efficient solution, with a considerable analytical involvement, but presenting some advantages when compared to purely numerical schemes. The characteristic of automatic global error control inherent to this technique allows for the computation of benchmark results as well. In this case, the integral transformation of the hyperbolic partial differential equation yields an infinite system of coupled ordinary differential equations of second order, which is then solved through well-established routines appropriate for handling initial value problems with stiff characteristics, such as the DIVPAG routine from the IMSL Library (1991). Numerical results are then produced for the temperature field within representative ranges of the governing parameters, and critically compared with those previously presented in the literature.

2. ANALYSIS

One-dimensional hyperbolic heat conduction in a fin with form of frustum of right circular cone is considered, initially at the temperature distribution $T_o(x)$, assuming constant properties as thermal conductivity (k), thermal diffusivity (α) and specific heat (c_p), and no internal heat generation. The fin tip is maintained insulated, while its larger surfaces are exchanging heat by convection with a fluid kept at a constant temperature, T_∞ and heat transfer coefficient varying with the time and the space, h(x,t). The fin base is subjected to a uniform prescribed temperature.

The general one-dimensional energy equation for the fin is written in the following form:

$$-A(x)\frac{\partial q''(x,t)}{\partial x}-q''(x,t)\frac{\partial A(x)}{\partial x}-h(x,t)\frac{dS(x)}{dx}[T(x,t)-T_\infty]=\rho C_p\frac{\partial T(x,t)}{\partial t}A(x) \qquad (1)$$

where A(x) is the area of the cross-section of the infinitesimal element of the fin, S(x) is the lateral area related to a perimeter p(x) and q"(x,t) is the heat flux in the fin.

For the phenomenon involving finite speed of propagation of the thermal waves, the classical Fourier model must be modified. Therefore, Cattaneo (1958) and Vernotte (1958) independently derived a model of heat flow in the form:

$$q''(x,t)=-k\frac{\partial T(x,t)}{\partial x}-\tau\frac{\partial q''(x,t)}{\partial t} \qquad (2)$$

where τ is the relaxation time of the material in which the heat conduction process is occurring. Combining Eq. (2) with Eq. (1), it then results the partial differential equation that governs the hyperbolic heat conduction in a convective fin, as:

$$\begin{aligned}&\rho C_p\tau\frac{\partial^2 T(x,t)}{\partial t^2}A(x)+\rho C_p\frac{\partial T(x,t)}{\partial t}A(x)+\tau\frac{dS(x)}{dx}\frac{\partial}{\partial t}\big[h(x,t)[T(x,t)-T_\infty]\big]=\\&kA(x)\frac{\partial^2 T(x,t)}{\partial x^2}+k\frac{\partial A(x)}{\partial x}\frac{\partial T(x,t)}{\partial x}-\frac{dS(x)}{dx}h(x,t)\frac{\partial}{\partial t}[T(x,t)-T_\infty]\end{aligned} \qquad (3)$$

Equation (3) describes the heat propagation in a convective fin with speed $\nu = (\alpha/\tau)^{1/2}$. Equation (4) is then written in dimensionless form as:

$$\tau_r K(X)\frac{\partial^2\theta^*(X,\xi)}{\partial\xi^2}+F(X,\xi)\frac{\partial\theta^*(X,\xi)}{\partial\xi}=\frac{\partial}{\partial x}\left[K(X)\frac{\partial\theta^*(X,\xi)}{\partial\xi}\right]-M^2G(X,\xi)\theta^*(X,\xi) \qquad (4a)$$

$$F(X,\xi)=K(X)+\tau_r M^2 W(X,\xi)$$

$$G(X,\xi)=\tau_r\frac{\partial W(X,\xi)}{\partial\xi}+W(X,\xi)$$

subjected to the following initial and boundary conditions:

$$\theta^*(X,0)=\theta_o^*(X)\,;\; X_b\le X\le X_t \qquad (4b)$$

$$\frac{\partial\theta^*(X,0)}{\partial\xi}=0\,;\; X_b\le X\le X_t \qquad (4c)$$

$$\theta^*(X_b,\xi)=1\,;\;\xi>0 \qquad (4d)$$

$$\frac{\partial\theta^*(X_t,\xi)}{\partial X}=0\,,\;\xi>0 \qquad (4e)$$

The following dimensionless groups were employed in obtaining Eqs. (4):

$$\begin{aligned}&X=x/l_r;\quad K(X)=A(x)/A_r;\quad \xi=\alpha t/l_r^2;\quad \tau_r=\alpha\tau/l_r^2;\quad \theta^*(X,\xi)=[T(x,t)-T_\infty]/[T_b-T_\infty];\quad M^2=m^2l_r^2\\&\theta_o^*(X)=[T_o(x)-T_\infty]/[T_b-T_\infty];\quad m^2=\frac{h_rP_r}{kA_r};\quad W(X,\xi)=\frac{h(x,t)}{P_rh_r}\frac{dS(x)}{dx}\end{aligned} \qquad (5)$$

Equations (4) constitute a non-homogeneous problem, which have to be filtered in order to obtain a better computational performance in the integral transform method. For this purpose, the dimensionless temperature $\theta^*(X,\xi)$ is written in a separated form as follows:

$$\theta^*(X,\xi)=1+\theta(X,\xi) \qquad (6)$$

Introducing Eq. (6) into Eqs. (4), to obtain the partial differential equation for the filtered potential $\theta(\eta,\xi)$ and filtered boundary conditions as:

$$\tau_r K(X)\frac{\partial^2\theta(X,\xi)}{\partial\xi^2}+F(X,\xi)\frac{\partial\theta(X,\xi)}{\partial\xi}=\frac{\partial}{\partial x}\left[K(X)\frac{\partial\theta(X,\xi)}{\partial\xi}\right]-M^2G(X,\xi)\theta(X,\xi)-M^2G(X,\xi) \tag{7a}$$

$$\theta(X,0)=\theta_o^*(X)-1\,;\;X_b\le X\le X_t \tag{7b}$$

$$\frac{\partial\theta(X,0)}{\partial\xi}=0\,;\;X_b\le X\le X_t \tag{7c}$$

$$\theta(X_b,\xi)=0\;;\;\xi>0 \tag{7d}$$

$$\frac{\partial\theta(X_t,\xi)}{\partial X}=0\;;\;\xi>0 \tag{7e}$$

2.1. Application

A geometric arrangement of a frustum of right circular cone is considered to obtain the solution of the presented problem given by Eqs. (7). Figure 1 shows a truncated conical pin of length (l_1-l_o) and base are A_1, subjected to a constant base temperature and negligible heat exchange with the surroundings, through the tip at $x=l_o$. Initially, the fin has reached the steady state temperature distribution with a uniform heat transfer coefficient h_r. For t>0, a transient situation develops due to a time-varying heat transfer coefficient h(t), with h_r=h(0), as described in Cotta et al. (1993).

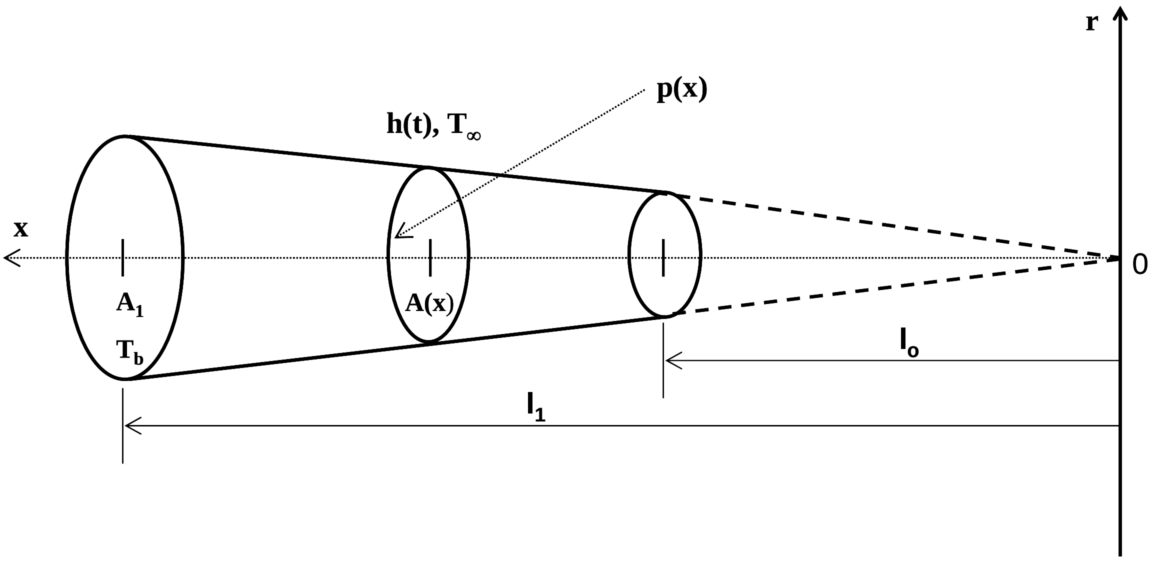

Figure 1. Geometric configuration ad coordinate system for the analysis of conical pin fin.

From direct comparison with the general system (5), we find:

$$X_b=l;\quad X_t=\frac{l_0}{l_1};\quad l_r=l_1;\quad A_r=A_1;\quad K(X)=X^2;\quad M^2=\frac{2h(0)l_1^2}{kr_1};\quad W(x,\xi)=\frac{h(\xi)}{h(0)}X \tag{8}$$

The time-dependent heat transfer coefficient is obtained from approximate expressions for mass flow rate decay typical of loss-of-flow accidents (Tong and Weisman, 1978), and given in the following functional form:

$$\frac{h(\xi)}{h(0)}=\frac{1}{1+B\xi} \tag{9}$$

2.2. Solution methodology

The next step is to find a solution for the potential $\theta(X,\xi)$, and for this purpose we follow the ideas in the GITT (Cotta, 1993; Cotta, 1994; Cotta and Mikhailov, 1997; Cotta and Mikhailov, 2006), first by selecting an appropriate auxiliary eigenvalue problem, which shall provide the basis for the eigenfunction expansion. Therefore, the following simple eigenvalue problem is here proposed:

$$\frac{d}{dX}\left[K(X)\frac{d\psi_i(X)}{dX}\right]+[\mu_i^2 K(X)-W_o(X)]\psi_i(X)=0 \tag{10a}$$

$$\psi_i(1)=0\,; \quad \frac{d\psi_i(X_t)}{dX}=0 \tag{10b,c}$$

Equations (10) can be analytically solved with $W_o(X) = 0$ to yield, respectively, the eigenfunctions and eigencondition for the determination of the eigenvalues (μ_i) as

$$\psi_i(X)=\frac{1}{X}\left[\sin(\mu_i X)-\tan(\mu_i)\cos(\mu_i X)\right] \tag{11}$$

$$\sin\left[\mu_i(1-X_t)\right]+\mu_i X_t\cos\left[\mu_i(1-X_t)\right]=0 \tag{12}$$

It can be shown that the eigenfunctions $\psi_i(X)$ present the following orthogonality property:

$$\int_1^{X_t} K(X)\psi_i(X)\psi_j(X)dX=\begin{cases}0, & i\neq j\\ N_i, & i=j\end{cases} \tag{13}$$

where N_i is the normalization integral. Also, one defines $\tilde{\psi}_i(X)$ as being the normalized eigenfunctions. Then, N_i and $\tilde{\psi}_i(X)$ are computed respectively as

$$N_i=\int_1^{X_t} K(X)\psi_i^2(X)dX \tag{14}$$

$$\tilde{\psi}_i(X)=\psi_i(X)/\sqrt{N_i} \tag{15}$$

Equations (11) and (14) together with the above properties allow the definition of the integral transform pair for the potential $\theta(X,\xi)$ as

$$\text{Transform: } \bar{\theta}_i(\xi)=\int_1^{X_t} K(X)\tilde{\psi}_i(X)\theta(X,\xi)dX \tag{16}$$

$$\text{Inverse: } \theta(X,\xi)=\sum_{i=1}^{\infty}\tilde{\psi}_i(X)\bar{\theta}_i(\xi) \tag{17}$$

To obtain the resulting system of differential equations for the transformed potentials $\bar{\theta}_i(\xi)$, the partial differential equation (7) is multiplied by $\tilde{\psi}_i(X)$, integrated over the domain $[X_b,X_t]$ in the X-direction, and the inverse formula, Eq. (17), is employed in place of the potential $\theta(X,\xi)$, resulting in the following transformed ordinary differential system:

$$\tau_r\frac{d^2\bar{\theta}_i(\xi)}{d\xi^2}+\sum_{j=1}^{\infty}A_{ij}(\xi)\frac{d\bar{\theta}_i(\xi)}{d\xi}+\sum_{j=1}^{\infty}F_{ij}(\xi)\bar{\theta}_i(\xi)=D_i(\xi), \quad i=1,2,3,... \tag{18}$$

The same operation can be performed over the initial conditions given by Eqs. (7b,c), to furnish

$$\bar{\theta}_i(0)=\int_1^{X_t} K(X)\tilde{\psi}_i(X)[\theta_o^*(X)-1]dX=\bar{f}_i \tag{19a}$$

$$\frac{d\bar{\theta}_i(0)}{d\xi}=0 \tag{19b}$$

The initial temperature distribution can be obtained from solving the steady-state version of Eq. (4), in the following way:

$$\frac{d}{dX}\left[X^2\frac{d\theta_o^*(X)}{dx}\right]-M^2X\theta_o^*(X)=0 \tag{20}$$

$$\theta_o^*(X)=\frac{1}{\sqrt{X}}\left[C_1I_1(2M\sqrt{X})+C_2K_1(2M\sqrt{X})\right] \tag{21}$$

$$C_1=\left[I_1(2M)+K_1(2M)\frac{I_2(2M\sqrt{X_t})}{K_2(2M\sqrt{X_t})}\right]^{-1} \tag{22}$$

$$C_2=\left[K_1(2M)+I_1(2M)\frac{K_2(2M\sqrt{X_t})}{I_2(2M\sqrt{X_t})}\right]^{-1} \tag{23}$$

where I_v and K_v are the modified Bessel functions.

The coefficients in Eqs. (18) are defined as follows:

$$A_{ij}(\xi)=\delta_{ij}+\frac{\tau_rM^2}{N_j}\frac{1}{(1+B\xi)}\int_1^{X_t}X\psi_i(X)\psi_j(X)dX\,;\ B_{ij}(\xi)=-\frac{B}{N_j}\frac{1}{(1+B\xi)^2}\int_1^{X_t}X\psi_i(X)\psi_j(X)dX \tag{24a,b}$$

$$C_{ij}(\xi)=\frac{1}{N_j}\frac{1}{(1+B\xi)}\int_1^{X_t}X\psi_i(X)\psi_j(X)dX\,;\ E_{ij}(\xi)=M^2[\tau_rB_{ij}(\xi)+C_{ij}(\xi)]\,;\ F_{ij}(\xi)=E_{ij}(\xi)+\delta_{ij}\mu_i^2 \tag{24c-e}$$

$$D_i(\xi)=-\frac{M^2}{\sqrt{N_i}}\left\{\frac{1}{(1+B\xi)}-\frac{\tau_rB}{(1+B\xi)^2}\right\}\int_1^{X_t}X\psi_i(X)dX\,;\quad \delta_{ij}=\begin{cases}0, & i\neq j\\ 1, & i=j\end{cases} \tag{24,f,g}$$

The coefficients may be analytically obtained through symbolic manipulation platforms such as the Mathematica system (Wolfram, 2003). Equations (18) form an infinite linear initial value problem, which has to be truncated in a sufficiently high order N, in order to compute the transformed potentials, $\bar{\theta}_i(\xi)$, to within a user prescribed accuracy target. For the solution of such a system, due to its expected stiff characteristics, specialized subroutines have to be employed, such as the subroutine DIVPAG from the IMSL Library (1991). This subroutine provides the important feature of automatic controlling the relative error over the solution of the ordinary differential equations system, allowing the user to establish error targets for the transformed potentials. Once this system is solved for the transformed potentials, the inverse formula, Eq. (17), is recalled to provide the potential $\theta(X,\xi)$, which is added to the Eq. (6), to furnish the complete temperature field.

3. RESULTS AND DISCUSSION

Numerical results for the temperature field were obtained from a code developed in the FORTRAN 90/95 programming language. The routine DIVPAG from the IMSL Library (1991) was used to numerically handle the truncated version of the system of ordinary differential equations, Eqs.(18) and (19), with a relative error target of 10^{-8} prescribed by the user, for the transformed potentials. The complete solution was computed using up to six hundreds terms ($N \leq 50$) in the eigenfunction expansion, and all the results were obtained with M = 1.0, X_t = 0.5, as well as different values of the governing parameters τ_r and B.

Tables 1 to 4 show the convergence behavior of the temperature distribution along the fin length with different dimensionless relaxation times, and different values of the parameter B and fixed values of dimensionless time. The columns solution for the temperature field through GITT, with different truncation orders, N, which demonstrate an excellent convergence rate even for N = 20 terms for dimensionless relaxation times τ_r = 0 and τ_r = 0.1, as seen in such tables. Also, Tables 1 and 2 brings a comparison of the present results with those of Cotta et al. (1993) showing an excellent agreement, with at least 3 significant digits. The possible difference among the results is attributed to different tolerance employed in the solution of the ODEs system.

Table 1. Comparison and convergence behavior of the present results for τ_r = 0, B=1, ξ=0.01, 0.1 and 1.

X	τ_r=0, B=1, M=1, ξ=0.01				
	N=5	**N=10**	**N=20**	**N=50**	**Cotta et al. (1993)**
	θ(X,ξ)				
0.500	0.88624	0.88635	0.88633	0.88633	0.88542
0.625	0.89749	0.89742	0.89742	0.89743	0.89686
0.750	0.92356	0.92352	0.92354	0.92354	0.92372
0.875	0.95855	0.95870	0.95869	0.95869	0.95970
X	**τ_r=0, B=1, M=1, ξ=0.1**				
	N=5	**N=10**	**N=20**	**N=50**	**Cotta et al. (1993)**
	θ(X,ξ)				
0.500	0.89120	0.89130	0.89129	0.89128	0.88981
0.625	0.90201	0.90194	0.90194	0.90194	0.90114
0.750	0.92706	0.92703	0.92704	0.92704	0.92750
0.875	0.96059	0.96072	0.96071	0.96071	0.96203
X	**τ_r=0, B=1, M=1, ξ=1.0**				
	N=5	**N=10**	**N=20**	**N=50**	**Cotta et al. (1993)**
	θ(X,ξ)				
0.500	0.93859	0.93865	0.93864	0.93864	0.93818
0.625	0.94475	0.94471	0.94471	0.94471	0.94446
0.750	0.95897	0.95895	0.95896	0.95896	0.95910
0.875	0.97789	0.97796	0.97796	0.97796	0.97837

Table 2. Comparison and convergence behavior of the present results for τ_r = 0, B=10, ξ=0.01, 0.1 and 1.

X	τ_r=0, B=10, M=1, ξ=0.01				
	N=5	**N=10**	**N=20**	**N=50**	**Cotta et al. (1993)**
	θ(X,ξ)				
0.500	0.88690	0.88701	0.88699	0.88699	0.88613
0.625	0.89808	0.89802	0.89802	0.89802	0.89748
0.750	0.92407	0.92403	0.92405	0.92405	0.92422
0.875	0.95896	0.95909	0.95908	0.95909	0.96005
X	**τ_r=0, B=10, M=1, ξ=0.1**				
	N=5	**N=10**	**N=20**	**N=50**	**Cotta et al. (1993)**
	θ(X,ξ)				
0.500	0.91824	0.91830	0.91829	0.91829	0.91761
0.625	0.92654	0.92650	0.92650	0.92650	0.92614
0.750	0.94592	0.94591	0.94592	0.94591	0.94613
0.875	0.97141	0.97149	0.97148	0.97148	0.97207
X	**τ_r=0, B=10, M=1, ξ=1.0**				
	N=5	**N=10**	**N=20**	**N=50**	**Cotta et al. (1993)**
	θ(X,ξ)				
0.500	0.98802	0.98803	0.98803	0.98803	0.98801
0.625	0.98923	0.98922	0.98922	0.98922	0.98922
0.750	0.99203	0.99203	0.99203	0.99203	0.99204
0.875	0.99573	0.99575	0.99575	0.99575	0.99576

Table 3. Convergence behavior of the temperature field along the fin length for a fixed dimensionless time and τ_r = 0.1 and B=1.

X	**τ_r=0.1, B=1, M=1, ξ=2**				
	N=10	**N=20**	**N=30**	**N=40**	**N=50**
	$\theta(X,\xi)$				
0.50	0.42194	0.42173	0.42173	0.42173	0.42173
0.55	1.24530	1.24550	1.24550	1.24550	1.24550
0.60	0.67133	0.67117	0.67116	0.67116	0.67116
0.65	0.94256	0.94271	0.94270	0.94270	0.94270
0.70	1.01390	1.01370	1.01370	1.01370	1.01370
0.75	0.69843	0.69857	0.69857	0.69857	0.69857
0.80	1.20910	1.20900	1.20900	1.20900	1.20900
0.85	0.67934	0.67941	0.67941	0.67941	0.67941
0.90	1.17280	1.17280	1.17280	1.17280	1.17280
0.95	0.87142	0.87147	0.87146	0.87146	0.87146

Table 4. Convergence behavior of the temperature field along the fin length for a fixed dimensionless time and τ_r = 0.1 and B=10.

X	**τ_r=0.1, B=10, M=1, ξ=2**				
	N=10	**N=20**	**N=30**	**N=40**	**N=50**
	$\theta(X,\xi)$				
0.50	0.79553	0.79549	0.79549	0.79549	0.79548
0.55	0.94160	0.94164	0.94164	0.94164	0.94164
0.60	0.84615	0.84612	0.84612	0.84612	0.84612
0.65	0.90095	0.90099	0.90098	0.90099	0.90098
0.70	0.92282	0.92279	0.92279	0.92279	0.92279
0.75	0.87844	0.87848	0.87848	0.87848	0.87848
0.80	0.97970	0.97967	0.97967	0.97966	0.97966
0.85	0.90032	0.90035	0.90035	0.90035	0.90035
0.90	1.00030	1.00030	1.00030	1.00030	1.00030
0.95	0.96235	0.96239	0.96238	0.96239	0.96239

Inspecting Fig. 2 one can analyze the influence of the dimensionless relaxation time on the temperature field along the fin length. The governing parameters utilized were B = 1.0 and 10, ξ = 2.0 and τ_r = 0 and 0.1. As can be seen from this figure, for dimensionless relaxation time equal to zero, the thermal wave propagates very fast, as a result of the speed of propagation approaching infinity, on the other hand, for the dimensionless relaxation time equal to 0.1, the thermal wave travels more slowly than for τ_r = 0. It is observed for τ_r = 0.1 that with the increase of the parameter B the amplitude of the temperature profile decreases. Such result, it was expected because the parameter B is inversely proportional to the heat transfer coefficient h, according to the Eq. (9). As smaller the value of B, larger values for h are expected, and therefore the thermal change is more intense, as verified by the higher temperature profiles.

From Fig. 3 one can also analyze the influence of the dimensionless relaxation time on the temperature field along the fin length. The governing parameters utilized were B = 1.0 and 10, ξ = 2.0 and τ_r = 1 and 5.0. As observed from this figure, for these dimensionless relaxation times, the results does not present any physical meaning, in function of extremely negative values for the temperature distribution. Such explanation may be because the present hyperbolic Cattaneo-Vernotte model presents an inconsistency with the second law of thermodynamics.

Figure 4 shows the behavior of the Fourier heat conduction model on the temperature field at the fin tip by varying the dimensionless time. From this figure, such analysis demonstrates that for τ_r = 0, the temperature at the fin tip rapidly increases with the dimensionless time, as expected, because this value of τ_r agrees with the classical Fourier model, in which the thermal waves are propagated with an infinite speed. As also can be seen from this figure, with the increase of the parameter B the heat transfer coefficient decreases and therefore the thermal exchange in the fin is less intensified, as it can be observed by the dashed line of this figure, and consequently the temperature rises more quickly for this situation.

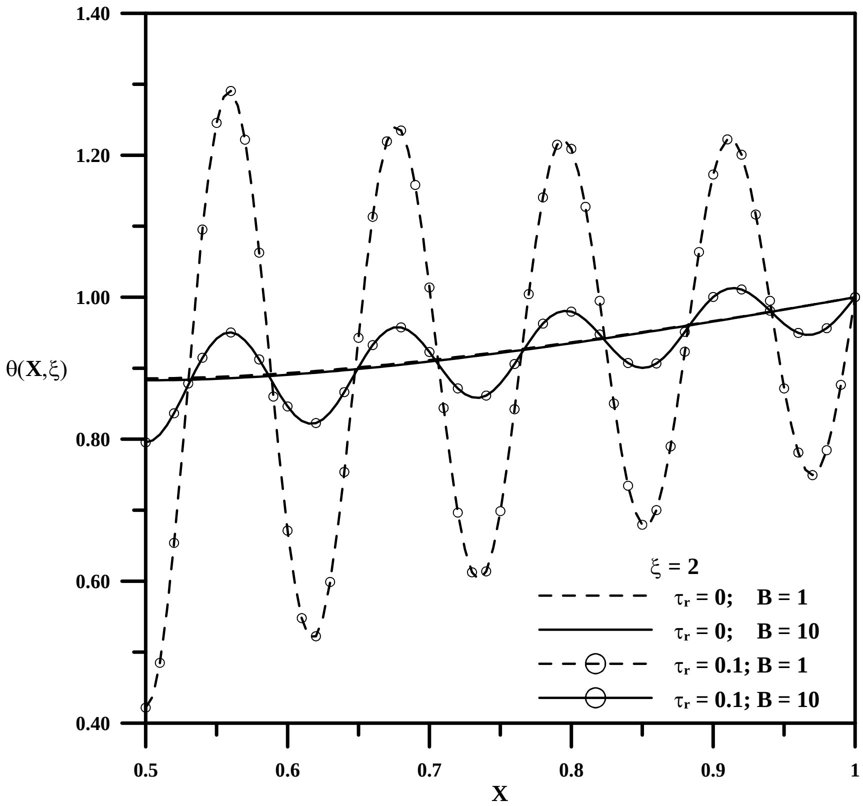

Figure 2. Temperature distribution along the fin length for different values of the parameter B, τ_r = 0 and 0.1 and ξ = 2.0.

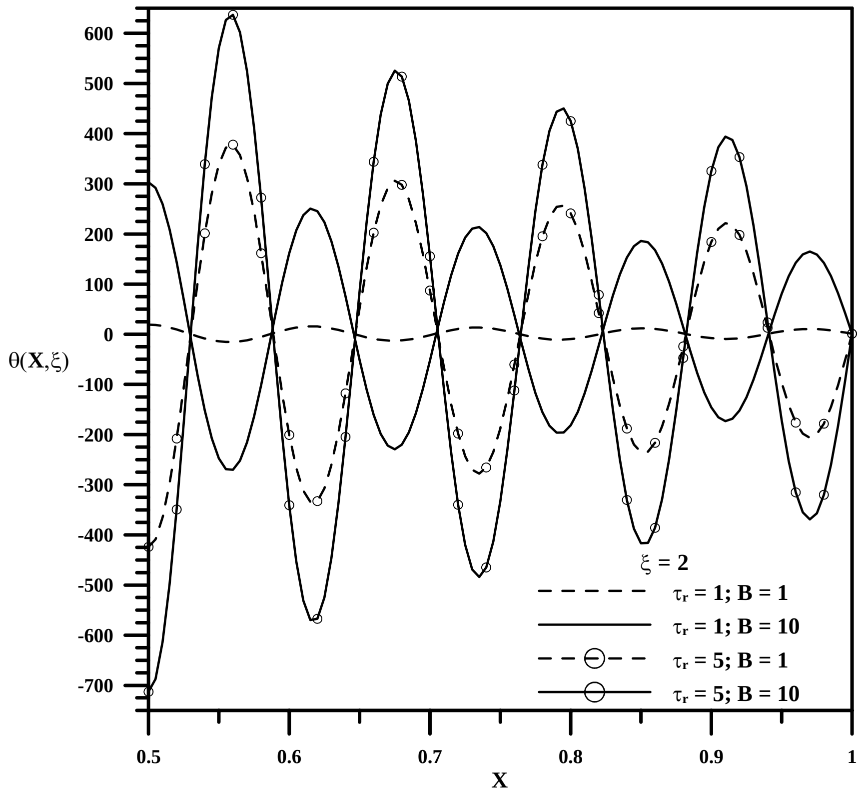

Figure 3. Temperature distribution along the fin length for different values of the parameter B, τ_r = 1.0 and 5.0 and ξ = 2.0.

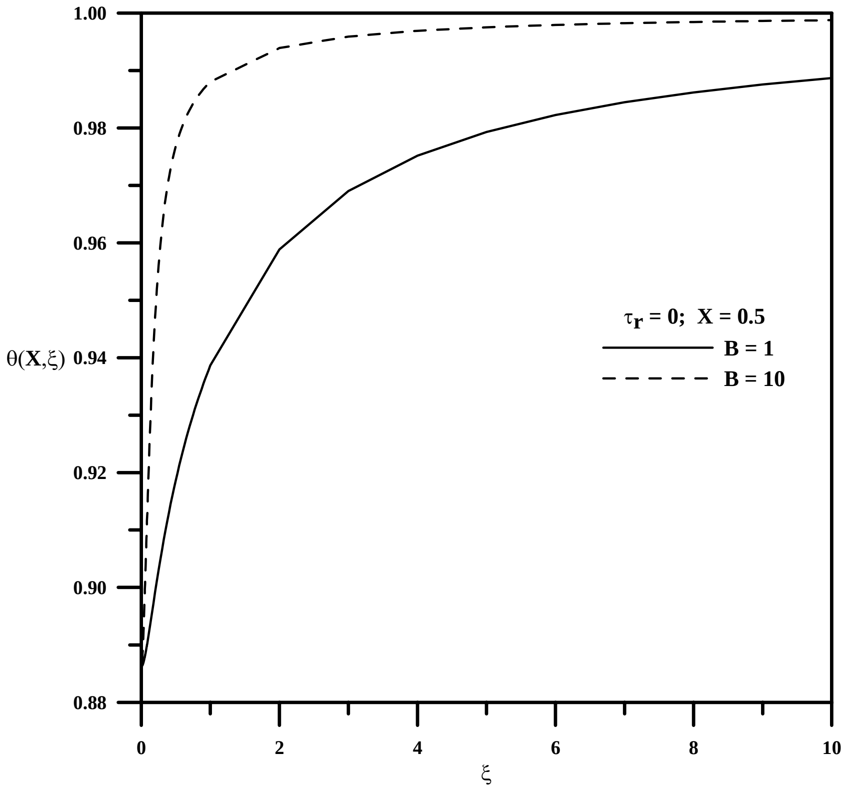

Figure 4. Temperature evolution at the fin tip (X = 0.5) and for dimensionless relaxation time (τ_r = 0).

4. CONCLUSIONS

Hyperbolic heat conduction for a convective conical pin fin, submitted to a time-dependent heat transfer coefficient, has been analyzed using the Generalized Integral Transform Technique (GITT). The complete solution was numerically obtained through the DIVPAG subroutine from the IMSL Library (1991) with an error-controlled procedure, offering reliable results for the fin temperature distribution with different governing parameters. It was verified that the GITT approach solves the hyperbolic heat conduction equation accurately; capturing the numeric jump discontinuities that are characteristics of hyperbolic problems generated by non-Fourier effects.

5. ACKNOWLEDGEMENTS

The authors would like to acknowledge the financial support provided by CNPq and FAPERJ.

6. REFERENCES

Bai, C. and Lavine, A.S., 1995, “On Hyperbolic Heat Conduction and Second Law of Thermodynamics”, Journal of Heat Transfer, Vol. 117, pp. 256-263.

Cattaneo, C., 1958, “Sur une Forme de L'équation de la Chaleur Eliminant le Paradoxe d´une Propagation Instantanée”, Comptes Rendus Hebdomadaires des Seances de L’Academie des Sciences, Vol. 247, pp. 431-433.

Cotta, R.M., 1993, “Integral Transforms in Computational Heat and Fluid Flow”, CRC Press, Boca Raton, USA.

Cotta, R.M., Santos, C.F.M., and Aparecido, J.B., 1993, “Transient Fin Analysis with Time-dependent Surface Dissipation”, Latin American Applied Research, Vol. 23, pp. 11-18.

Cotta, R.M., 1994, “Benchmark Results in Computational Heat and Fluid Flow: - The Integral Transform Method”, Int. J. Heat Mass Transfer (Invited Paper), Vol. 37 (Suppl. 1), pp. 381-393.

Cotta, R.M. and Mikhailov, M.D., 1997, “Heat Conduction: Lumped Analysis, Integral Transforms, Symbolic Computation”, Wiley-Interscience, USA.

Cotta, R.M. and Mikhailov, M.D., 2006, “Hybrid Methods and Symbolic Computations”, in: Handbook of Numerical Heat Transfer, 2nd edition, Chapter 16, Eds. W.J. Minkowycz, E.M. Sparrow, and J.Y. Murthy, John Wiley, New York, pp. 493-522.

Criado-Sancho, M. and Llebot, J.E., 1993, “Behavior of Entropy in Hyperbolic Heat Conduction”, Physical Review E, Vol. 47, pp. 4104-4107.

Cruz, A.G.B., Macêdo, E.N. and Quaresma, J.N.N., 2001, “One-dimensional Hyperbolic Heat Conduction Analysis through Finite Volume and Gear Methods”, Proceedings of 16th Brazilian Congress of Mechanical Engineering, Uberlândia, Brazil, Paper code TRB0071.

IMSL Library, 1991, Math/Lib, Houston, Texas.

Lin, J. Y., 1998, “The non-Fourier Effect on the Fin Performance under Periodic Thermal Conditions”, J. Applied Mathematical Modelling, Vol. 22, pp. 629-640.

Macêdo, E.N., Monteiro, E.R. and Quaresma, J.N.N., 2005, “One-Dimensional Hyperbolic Heat Conduction Analysis through Integral Transform Method”, Proceedings of the 4th International Conference on Computational Heat and Mass Transfer, Paris-Cachan, France.

Quaresma, J.N.N., Macêdo, E.N. and Cruz, A.G.B., 2001, “Hybrid Solution in Hyperbolic Heat Conduction: Laplace Transform with Numerical Inversion”, Proceedings of the 2nd International Conference on Computational Heat and Mass Transfer, Rio de Janeiro, Brazil.

Silva, C.A.M., Macêdo, E.N., Quaresma, J.N.N. and Cotta, R.M., 2006, “Analysis of Hyperbolic Fins through the Generalized Integral Transform Technique”, Proceedings of the 11th Brazilian Congress of Thermal Sciences and Engineering -- ENCIT 2006, Curitiba, Brazil, Paper CIT06-0654.

Tong, L.S., and Weisman, J., 1978, “Thermal Analysis of Pressurized Water Reactors”, American Nuclear Society.

Tsai, C.S., Lin, Y.C. and Hung, C.I., 2005, “A Study on the non-Fourier Effects in Spherical Media due to Sudden Temperature Changes on the Surfaces”, J. Heat and Mass Transfer, Vol.41, pp. 706-716.

Vernotte, P., 1958, “Les Paradoxes de la Theorie Continue de L'Équation de la Chaleur”, Comptes Rendus Hebdomadaires des Seances de L’Academie des Sciences, Vol. 246, pp. 3154-3155.

Wolfram, S., 2003, The Mathematica Book, 5th ed., Wolfram Media.

7. RESPONSIBILITY NOTICE

The authors are the only responsible for the printed material included in this paper.